PREPARATIONS AND CHARACTERIZATIONS OF CHITOSAN, ZnO NANOPARTICLE AND CHITOSAN-ZnO NANOCOMPOSITE

Kyu Kyu Aung[1], Khin Thida Htun[2]

Abstract

In this research, chitosan was prepared from *Metapenaeus dobosoni* species (Pezun-phyu) shrimp shell wastes by using a chemical method. The preparation of chitosan process consists of four steps such as deproteinization, demineralization, decolouration and deacetylation, respectively. The prepared chitosan (CS) was matched with FT IR and XRD reports of the standard chitosan. The prepared CS was also characterized by SEM. The yield percent of CS and the degree of acetylation were observed as 27.82 % and 72 %, respectively. The moisture and ash percentage of CS were observed to be 8.6 % and 0.2 %, respectively. The average crystallite size of the CS was 12.20 nm. The micrographs of CS showed the layers of flakes, porous and cage like morphology. The ZnO nanoparticle was prepared by co-precipitation method. It was characterized by TG-DTA, XRD, FT IR and SEM. The average crystallite size of the prepared ZnO nanoparticle was 20.99 nm. According to the SEM, the prepared ZnO nanoparticle showed spherical shape, porous structure and irregular surface morphology. And then chitosan-ZnO (CS-ZnO) nanocomposite was also prepared by using co-precipitation method. The prepared CS-ZnO nanocomposite was characterized by XRD, FT IR and SEM techniques. The average crystallite size of prepared CS-ZnO nanocomposite was 13.78 nm. In the present study, antimicrobial activities on chitosan (CS), ZnO nanoparticles and prepared chitosan-ZnO (CS-ZnO) nanocomposite were compared.

Keyword: Shrimp shell wastes, chitosan, ZnO nanoparticle, chitosan-ZnO nanocomposite, antimicrobial activities

Introduction

Shrimp is one of the important fisheries products worldwide including Myanmar. After the process of separation of the head and shells, this product is mostly exported in frozen condition. Head and shell materials of shrimp have only a low economic value and are treated as bio-waste or sold to animal feed manufactures. About 50 % of shrimp total body weight is waste. Shrimp wastes are environmental contaminants. Therefore, utilization of these wastes can prevent environmental contamination. This bio-waste can be used to produce valuable products such as chitin. Chitin is the second most abundant biopolymers found in nature after cellulose. Chitin $(C_6H_{11}O_4N)_n$ is a liner polysaccharide consisting of β(1-4)-linked 2-acetamido- 2-deoxy-D-glucopyranose. Chitosan is the most important derivative of chitin after deacetylation (Pokhrel *et al*., 2015). Chitosan is a linear polysaccharide consisting of β (1-4)-linked 2-amino-2-deoxy-D--glucopyranose. It is insoluble in water but soluble inorganic acids and organic acid. It is the universally accepted non-toxic chitosan. Chitosan is very reactive because of its free amino groups (Younes and Rinaudo, 2015). The difference between chitosan and cellulose is the amine ($-NH_2$) group in the position C-2 of chitosan instead of the hydroxyl (-OH) group found in cellulose. However, unlike plant fiber, chitosan possesses positive ionic charges (amino group), which give it the ability to chemically bind with negatively charged fats, lipids, cholesterol, metal ions, proteins and macromolecules (Bui *et al*., 2017).

The ZnO nanoparticles can be prepared by many synthetic methods such as co-precipitation, sol-gel, hydrothermal method etc. This nanoparticles can potentially be applied to gas sensors, photocatalyst for degradation of waste water pollutants, catalysts,

[1] Dr, Associate Professor, Department of Engineering Chemistry, Technological University (Pathein)
[2] Dr, Associate Professor, Department of Chemistry, Myeik University

semiconductors, piezoelectric devices, field-emission displays, ultraviolet photodiodes, surface accoustic wave devices, UV-shielding materials, rubber, medical and dental materials, pigments and coatings, ceramic, concrete, antibacterial and bactericide, and composites (Salahuddin *et al*., 2015). The antimicrobial activity of the ZnO nanoparticles is known to be a function of the surface area in contact with the microorganisms. Large surface area of the nanoparticles enhances their interaction with the microbes to carry out a broad range of probable antimicrobial activities (Espitia *et al*., 2012).

Chitosan (CS) along with metal oxide nanoparticles has been utilized as a stability agent due to its excellent film-forming ability, mechanical strength, biocompatibility, non-toxicity, high permeability towards water, susceptibility to chemical modifications and antibacterial (Kavitha and Subashini, 2015). Chitosan also acts as a chelating agent that selectively binds trace metals and metal oxide, thereby inhibit the production of toxins and microbial growth.

Materials and Methods

Preparation of Chitosan (CS)

In the present work, preparation of chitin from *Metapenaeus dobosoni* species shrimp shell wastes were collected from Myoma market at Thanlyin in yangon Division. These wastes were washed several times with water and then dried at room temperature. Chitin was prepared by three steps such as demineralization with 4% HCl, deproteinization with 3% NaOH and decolouration with acetone by using chemical method. And then the chitosan was obtained by deacetylation of chitin by 50% NaOH (Bui *et al*., 2017). The prepared CS was characterized by FT IR, XRD and SEM.

Preparation of ZnO Nanoparticle

In the present work, ZnO nanoparticle was prepared. 150 mL of 0.05 M zinc nitrate solution was added in 1L beaker. Then, 0.1M NaOH solution was slowly added with continuous stirring using magnetic stirrer, until pH of the mixture solution is 9 by using co-precipitation method. And then, the $Zn(OH)_2$ precipitate was filtered and washed with distilled water until neutral pH. The precipitate was dried at 70^{o}C at 24 h and then calcined at 400 ^{o}C in furnace. The ZnO nanoparticle was obtained. The ZnO nanoparticle was characterized by TG-DTA, XRD, FT IR and SEM.

Preparation of Chitosan-Zinc Oxide Nanocomposite

The Chitosan-Zinc Oxide (CS-ZnO) nanocomposite was prepared by co-precipitation method. Firstly, 3 g of ZnO nanoparticle was dissolved in 2% acetic acid and 1 g of CS was dissolved in 2% acetic acid by stirring using magnetic stirrer at pH is 4. These solutions were mixed with continuous stirring until it becomes clear solution. While stirring, 0.05 M NaOH solution was added drop wise until pH of solution is to be 9. The white precipitate of Chitosan-Zinc Oxide (CS-ZnO) was obtained. It was filtered and dried at 60^{o}C for 1 h. The prepared CS-ZnO nanocomposite was characterized by FT IR, XRD and SEM.

Determination of Antimicrobial Activities on Chitosan (CS), ZnO Nanoparticle and Chitosan-Zinc Oxide Nanocomposite

The chitosan, ZnO nanoparticle and Chitosan-Zinc Oxide (CS-ZnO) nanocomposite were tested against four pathogenic bacteria: two gram-positive (*Staphylococcus aureus* and *Bacillus*

subtilis), two gram-negative (*Pseudomonas aeruginosa* and *Escherichia coli*), one pathogenic yeast (*Candida albicans*) and one fungi (*Aspergillus niger*) by agar well diffusion method**.**

Results and Discussion

Characterization of the Prepared Chitosan

In this research, the photograph of prepared CS from shrimp shell wastes is shown in Figure 1. The prepared CS was characterized by FT IR, XRD and SEM measurements.

Figure 1 Photograph of the prepared CS from shrimp shell wastes

FTIR analysis of the prepared chitosan

The FT IR spectrum of prepared CS is presented in Figures 2. The strong absorption bands around at 3460, 3360 and 3105 cm^{-1} are due to OH and amine N-H symmetrical stretching vibrations. The small peak around 2870 cm^{-1} was appeared due to CH stretching of $–CH_2–$ and $–CH_3$ groups. The peaks around at 1622 and 1552 cm^{-1} were indicated the C=O stretching of amide I and amide II. The major absorption band was observed at1151, 1077 and 1020 cm^{-1} which represents the free amino group $-NH_2$ at C-2 position of glucosamine, a major group present in CS. The peak around at 1375 and 1304 cm^{-1} represent the C-H bending vibrations of $–CH_2$ and amide III (Arafat *et al*, 2015; Knidri *et al.*, 2017). The degree of acetylation is calculated by using peaks at 3460 and 1655 in the FT IR data. The degree of acetylation of chitosan is 72%.

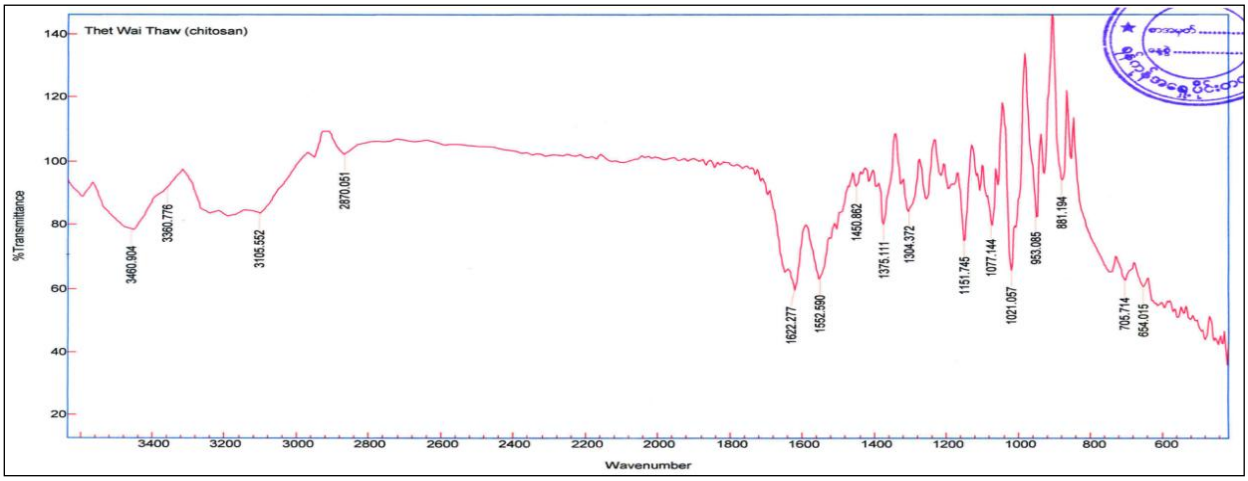

Figure 2 FTIR spectrum of the prepared CS from shrimp shell wastes

XRD analysis of the prepared chitosan

In this studies, the two peaks at 2 θ value around at 10.5º and 20º correspond to the (102) and (110) crystal planes indicating crystalline structure of chitosan (Knidri *et al.*, 2017). In the XRD data, Miller indices of chitosan were matched with JCPDS standard library data 03-0226.

Figure 3 shows the XRD diffractogram of prepared chitosan. Table 1 reveals the XRD data of chitosan. According to XRD data, the peaks at 2θ around 11º, 17º, 22º, 23º, 26º, 27º, 28º, 30º, 31º, 32º, 33º, 35º, 36º and 40º corresponding to (¯101), (¯102), (012), (¯202), (030), (031), (210), (003), (¯132), (013), (131), (¯232), (¯313) and (103) planes, respectively. The average crystallite size of chitosan was calculated by Debye-Scherrer equation. The average crystallite size of chitosan is 12.20 nm.

Table 1 The XRD Data of the prepared Chitosan from shrimp shell wastes

[chitosan-No3-MaThetWaiThaw-F296.raw] chitosan — Peak Search Report

SCAN: 10.0/70.0/0.02/0.12(sec), Cu(40kV,40mA), I(max)=160, 02/28/18 15:06

PEAK: 7-pts/Parabolic Filter, Threshold=1.0, Cutoff=0.1%, BG=1/1.0, Peak-Top=Parabolic Fit

NOTE: Intensity = Counts, 2T(0)=0.0(deg), Wavelength to Compute d-Spacing = 1.54056Å (Cu/K-alpha1)

#	2-Theta	d(Å)	(h k l)	BG	Height	Height%	Area	Area%	FWHM	XS(Å)	P/N
1	11.720	7.5445	(-1 0 1)	20	12	30.8	124	11.1	0.176	553	1.1
2	17.233	5.1415	(-1 0 2)	29	12	30.8	42	3.8	0.060	>1000	0.9
3	20.536	4.3213	(0 0 2)	69	24	61.5	861	76.9	0.610	134	1.2
4	20.707	4.2861	(1 0 1)	66	39	100.0	857	76.5	0.374	224	1.9
5	22.237	3.9945	(0 1 2)	51	11	28.2	144	12.9	0.223	407	0.7
6	23.356	3.8056	(-2 0 2)	50	23	59.0	642	57.3	0.475	175	1.3
7	26.075	3.4145	(0 3 0)	45	22	56.4	158	14.1	0.122	>1000	1.3
8	26.709	3.3349	(2 0 0)	43	10	25.6	109	9.7	0.185	523	0.7
9	27.741	3.2132	(0 3 1)	43	18	46.2	457	40.8	0.432	195	1.2
10	28.162	3.1661	(2 1 0)	47	13	33.3	199	17.8	0.260	341	0.8
11	30.985	2.8838	(0 0 3)	43	9	23.1	163	14.6	0.308	283	0.6
12	31.328	2.8529	(-1 3 2)	38	28	71.8	1120	100.0	0.680	123	1.7
13	32.734	2.7335	(0 1 3)	42	13	33.3	110	9.8	0.144	801	0.9
14	33.342	2.6850	(1 3 1)	39	12	30.8	399	35.6	0.565	149	0.8
15	35.242	2.5446	(-2 3 2)	32	15	38.5	285	25.4	0.323	271	1.1
16	35.999	2.4927	(0 4 1)	31	13	33.3	107	9.6	0.140	853	1.0
17	36.552	2.4563	(-3 1 3)	25	24	61.5	233	20.8	0.165	637	1.7
18	36.916	2.4329	(-3 1 1)	28	18	46.2	230	20.5	0.217	434	1.3
19	40.190	2.2419	(1 0 3)	32	15	38.5	330	29.5	0.374	235	1.1
20	40.921	2.2036	(0 4 2)	28	16	41.0	329	29.4	0.350	253	1.2

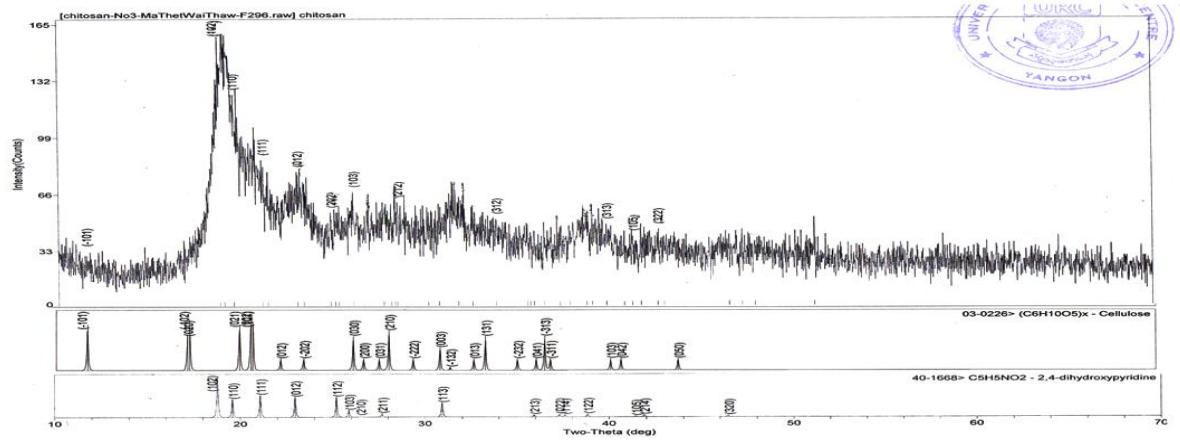

Figure 3 XRD diffractogram of the prepared CS from shrimp shell wastes

Morphological analysis of the prepared chitosan by SEM

The SEM micrograph of the prepared CS is presented in Figure 4. The prepared micrograph of CS shows the layers of flakes, porous and cage like morphology appeared on some areas.

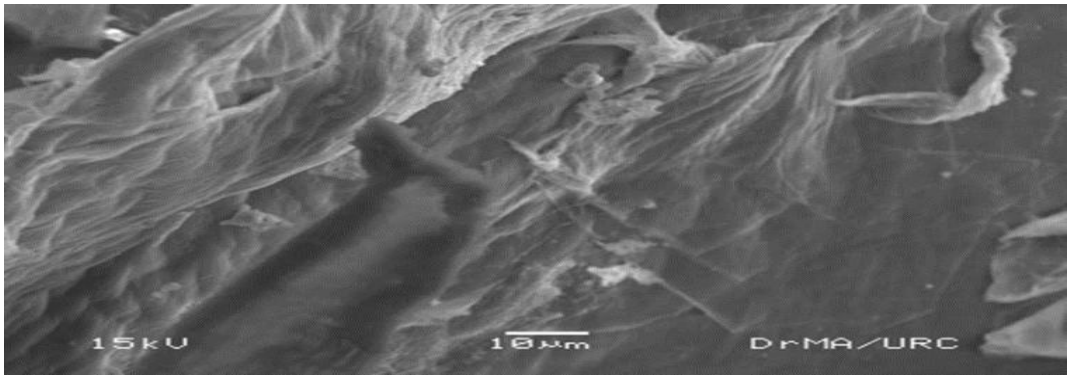

Figure 4 SEM micrograph of the prepared CS from shrimp shell wastes

Characterization of the Prepared ZnO nanoparticle

TG-DTA data of the prepared ZnO nanoparticle

The thermogravimetric curves demonstrated completely decomposition of sample at 30 to 600°C. The TG-DTA curves of prepared ZnO nanoparticle (zinc hydroxide) are illustrated in Figure 5(a). At low temperature, two endothermic peaks around 144.79 and 262.42 °C were due to loss of volatile surfactant molecules absorbed on the $Zn(OH)_2$ during synthesis conditions. At high, temperature, two peaks around 371 °C and 449 °C were assigned due to the decomposition of $Zn(OH)_2$ to ZnO. The percent of total weight loss was 11.021 %.

XRD analysis of the prepared ZnO nanoparticle

The X-ray powder Diffraction (XRD) measurement was carried out to confirm the crystallinity using Regaku X-ray diffractometer with Cu/Kα radiation (λ=1.54056 Å) in the range of 2 θ between 10º-70º. In XRD data, Miller indices of ZnO NP's were matched with ZnO from JCPDS standard library data 80-0075. Figure 5(b) showes the XRD diffractograms of ZnO nanoparticle. Table 2 reveales (a) the XRD data and (b) peaks ID Data of ZnO nanoparticle. According to the XRD data, the sharp peaks at 2 θ value around 31º; 34º, 36º, 47º, 56º, 62º, 67º and 69º are corresponding to (100), (002), (101), (102), (110), (103), (112) and (201) planes, respectively. All diffraction peaks of ZnO nanoparticle have hexagonal wurtzite structure. The average crystallite size was calculated by Debye-Scherrer equation. The average crystallite size of ZnO nanoparticle is 20.99 nm.

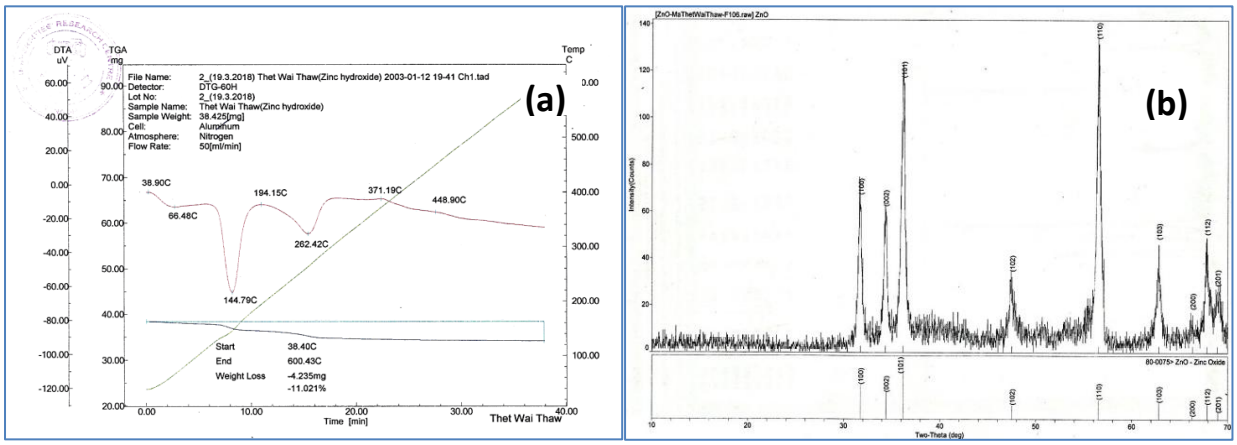

Figure 5 (a) TG-DTA thermogram of the prepared ZnO nanoparticle
(b) XRD diffractogram of the prepared ZnO nanoparticle

Table 2(a) XRD Data of the prepared ZnO nanoparticle

[ZnO-MaThetWaiThaw-F106.raw] ZnO — Peak Search Report

SCAN: 10.0/70.0/0.02/0.24(sec), Cu(40kV,40mA), I(max)=135, 01/25/18 23:32

PEAK: 9-pts/Parabolic Filter, Threshold=1.0, Cutoff=0.1%, BG=1/1.0, Peak-Top=Parabolic Fit

NOTE: Intensity = Counts, 2T(0)=0.0(deg), Wavelength to Compute d-Spacing = 1.54056Å (Cu/K-alpha1)

#	2-Theta	d(Å)	(h k l)	BG	Height	Height%	Area	Area%	FWHM	XS(Å)	P/N
1	31.712	2.8193	(1 0 0)	5	60	48.8	1492	47.7	0.423	201	3.7
2	34.321	2.6107	(0 0 2)	6	54	43.9	1230	39.4	0.387	222	3.5
3	36.157	2.4822	(1 0 1)	10	105	85.4	2765	88.5	0.448	192	4.9
4	47.480	1.9133	(1 0 2)	8	24	19.5	594	19.0	0.421	212	2.1
5	56.525	1.6267	(1 1 0)	9	123	100.0	3125	100.0	0.432	215	5.4
6	62.791	1.4786	(1 0 3)	6	40	32.5	840	26.9	0.357	272	2.9
7	66.318	1.4083	(2 0 0)	5	11	8.9	214	6.8	0.331	301	1.4
8	67.831	1.3805	(1 1 2)	10	38	30.9	850	27.2	0.380	261	2.7
9	68.933	1.3611	(2 0 1)	12	14	11.4	378	12.1	0.459	215	1.4

Table 2(b) Peaks ID Data of the prepared ZnO nanoparticle

[ZnO-MaThetWaiThaw-F106.raw] ZnO — Peak ID Report

SCAN: 10.0/70.0/0.02/0.24(sec), Cu(40kV,40mA), I(max)=135, 01/25/18 23:32

PEAK: 9-pts/Parabolic Filter, Threshold=1.0, Cutoff=0.1%, BG=1/1.0, Peak-Top=Parabolic Fit

NOTE: Intensity = Counts, 2T(0)=0.0(deg), Wavelength to Compute d-Spacing = 1.54056Å (Cu/K-alpha1)

#	2-Theta	d(Å)	Height	Height%	Phase ID	d(Å)	I%	(h k l)	2-Theta	Delta
1	31.712	2.8193	60	48.8	ZnO	2.8180	57.9	(1 0 0)	31.727	0.015
2	34.321	2.6107	54	43.9	ZnO	2.6049	44.2	(0 0 2)	34.400	0.079
3	36.157	2.4822	105	85.4	ZnO	2.4786	100.0	(1 0 1)	36.211	0.055
4	47.480	1.9133	24	19.5	ZnO	1.9128	22.9	(1 0 2)	47.493	0.013
5	56.525	1.6267	123	100.0	ZnO	1.6270	32.4	(1 1 0)	56.517	-0.008
6	62.791	1.4786	40	32.5	ZnO	1.4784	27.6	(1 0 3)	62.801	0.010
7	66.318	1.4083	11	8.9	ZnO	1.4090	4.4	(2 0 0)	66.281	-0.037
8	67.831	1.3805	38	30.9	ZnO	1.3799	24.3	(1 1 2)	67.864	0.033
9	68.933	1.3611	14	11.4	ZnO	1.3601	11.4	(2 0 1)	68.990	0.057

Line Shifts of Individual Phases:
PDF#80-0075 - Zinc Oxide <2T(0) = 0.0, d/d(0) = 1.0>

FT IR analysis of the prepared ZnO nanoparticle

In this research, FT IR analysis of prepared ZnO nanoparticle is presented in Figure 6(a). The peaks around 3400 cm^{-1} indicated the stretching vibration of hydroxyl groups on ZnO surface absorbed water vapour. The broad bands around 1600 cm^{-1} due to bending vibration of hydroxyl groups on ZnO surface absorbed water vapour. The metal oxides generally give absorption bands below 1000 cm^{-1} arising from interatomic vibrations. The bands around 860 and 450 cm^{-1} corresponded to O-Zn-O and Zn-O-Zn stretching and bending vibrations (Kumar and Rani, 2013).

SEM measurement of the prepared ZnO nanoparticle

In this study, the SEM micrograph of the prepared ZnO nanoparticle is presented in Figure 6(b). In the micrograph of the ZnO nanoparticle showed spherical shape, porous structure and irregular surface morphology.

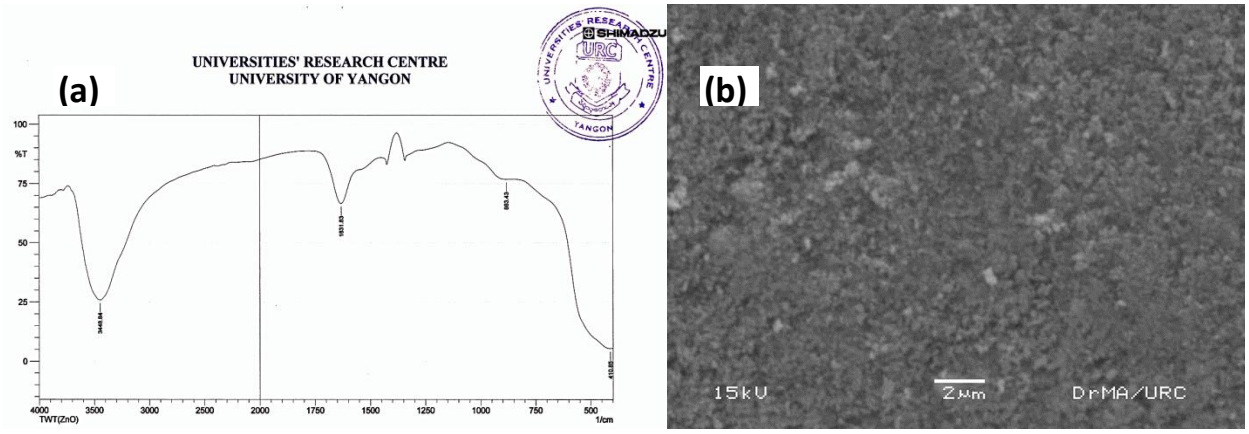

Figure 6 (a) FT IR spectrum of the prepared ZnO nanoparticle
(b) SEM micrograph of ZnO nanoparticle

Characterization of the Prepared Chitosan-Zinc Oxide (CS-ZnO) Nanocomposite

In this research, the prepared CS-ZnO nanocomposite is characterized by FT IR, XRD and SEM measurements.

FT IR analysis of the prepared CS-ZnO nanocomposite

In this research, FT IR analysis of the prepared CS-ZnO nanocomposite was carried out to characterize [Figure 7(a)]. The peak observed at 3425 cm^{-1} to the stretching vibration of $–NH_2$ group and –OH group. The C-H stretching vibration was observed at 2878 cm^{-1}. The peak 1628 cm^{-1} indicated the amine I group (C-O stretching along the N-H deformation mode). The peak 1589 cm^{-1} was assigned to the –NH deformation mode. The band around 1383 and 1332 cm^{-1} were showed C-H in plane bending vibrational group. The peak around 1157 cm^{1} showed a small shoulder peak of ß (1-4) glycosidic band in polysaccharide unit and around 1065 cm^{-1} indicated the stretching vibration of C-O-C in glucose circle. The band observed in the range of 575-532 cm^{-1} corresponds to the stretching vibration of N-Zn-O group (Dhanavel *et al.*, 2014 and Demir *et al*., 2016).

XRD analysis of the prepared CS-ZnO nanocomposite

In this studies, X-ray Powder Diffraction (XRD) measurement was carried out to confirm the crystallinity using Rigaku X-ray diffractometer with Cu/Ka radiation (λ= 1.54056 Å) in the range of 2 θ between 10º-70º. The two peaks at 2θ values around at 10.5° and 20° correspond to the crystal panes indicating crystalline structure of CS (Dhannavel *et al.*, 2014). According to the XRD data, the sharp peaks at 2θ value around 31°, 34°, 36°, 47°, 56°, 62°, 66°, 67° and 69° are corresponding to (1 0 0), (0 0 2), (1 0 1), (1 0 2), (1 1 0), (1 0 3), (2 0 0), (1 1 2) and (2 0 1) planes, respectively. Figure 7(b) shows the XRD diffractograms of prepared CS-ZnO nanocomposites. Table 3 shows the XRD data of prepared CS-ZnO nanocomposites. The average crystallite size of prepared CS-ZnO nanocomposites is 13.78 nm.

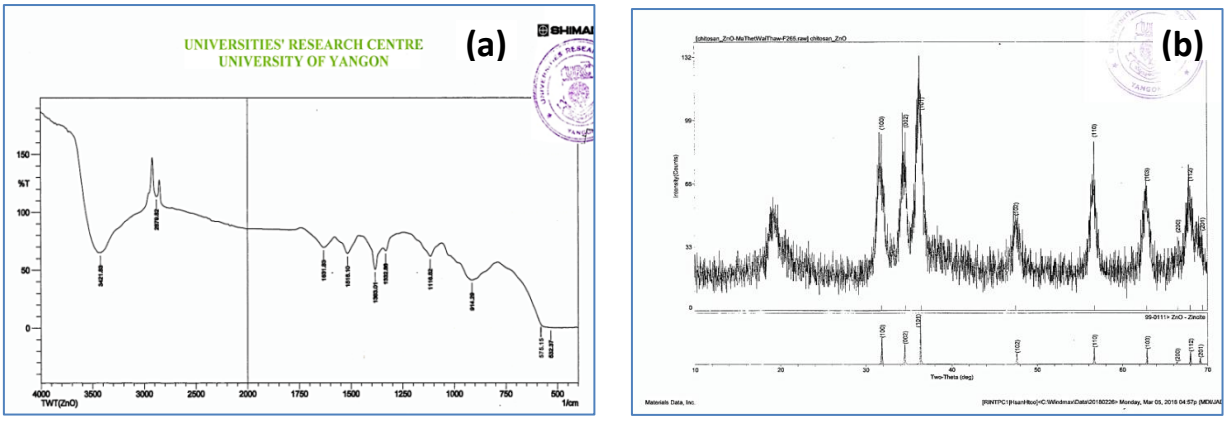

Figure 7 (a) FT IR spectrum of the prepared CS-ZnO nanocomposite
(b) XRD diffractogram of the prepared CS-ZnO nanocomposite

SEM measurement of the prepared CS-ZnO nanocomposite

The SEM micrograph of the prepared CS-ZnO nanocomposite is presented in Figure 8. In the micrograph of the prepared CS-ZnO nanocomposite showed cage like morphology indicating uniformly dispersion of ZnO nanoparticles into CS.

Table 3 XRD Data of the prepared CS-ZnO nanocomposite

[chitosan_ZnO-MaThetWaiThaw-F265.raw] chitosan_ZnO											Peak Search Report
SCAN: 10.0/70.0/0.02/0.12(sec), Cu(40kV,40mA), I(max)=133, 02/26/18 14:07											
PEAK: 9-pts/Parabolic Filter, Threshold=1.0, Cutoff=0.1%, BG=1/1.0, Peak-Top=Parabolic Fit											
NOTE: Intensity = Counts, 2T(0)=0.0(deg), Wavelength to Compute d-Spacing = 1.54056Å (Cu/K-alpha1)											
#	2-Theta	d(Å)	(h k l)	BG	Height	Height%	Area	Area%	FWHM	XS(Å)	P/N
1	31.781	2.8133	(1 0 0)	24	68	100.0	2413	83.4	0.603	139	3.5
2	34.564	2.5929	(0 0 2)	37	56	82.4	1314	45.4	0.399	215	2.9
3	36.416	2.4651	(1 0 1)	38	64	94.1	2895	100.0	0.769	110	3.2
4	47.467	1.9138	(1 0 2)	21	26	38.2	1144	39.5	0.748	117	1.9
5	56.674	1.6228	(1 1 0)	23	65	95.6	1749	60.4	0.457	202	3.5
6	62.896	1.4764	(1 0 3)	20	45	66.2	1795	62.0	0.678	139	2.8
7	66.536	1.4042	(2 0 0)	22	16	23.5	264	9.1	0.280	363	1.3
8	67.986	1.3777	(1 1 2)	28	37	54.4	1177	40.7	0.541	180	2.3
9	69.408	1.3530	(2 0 1)	24	15	22.1	408	14.1	0.462	214	1.2

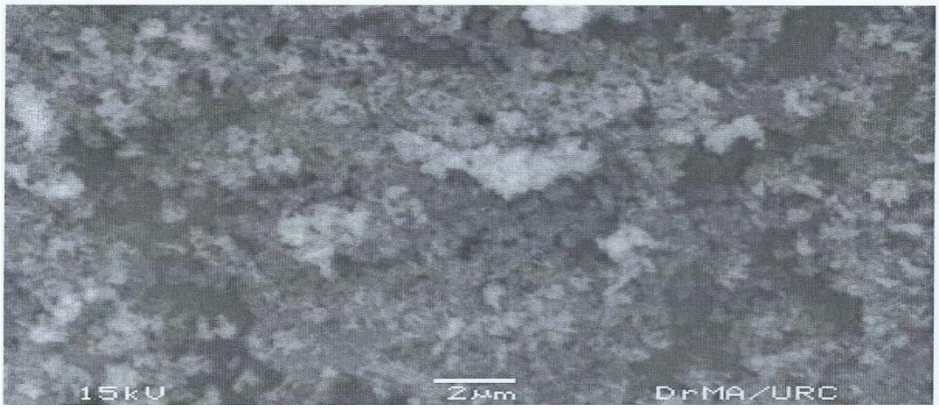

Figure 8 SEM micrograph of the prepared CS-ZnO nanocomposite

Antimicrobial Activities of Chitosan, ZnO Nanoparticle and the Prepared Chitosan-ZnO Nanocomposite

The antimicrobial activity of CS, ZnO NP's and the prepared CS-ZnO nanocomposite were tested against four pathogenic bacteria, two gram negative (*Pseudomonas aeruginos* and *Esherichia coli*), two gram positive (*Staphylococcus aureus* and *Bacillus subtilis*), one pathogenic yeast (*Candida albican*) and one fungi (*Asperigillus niger*) in Figure 9 and Table 4.

The CS against different groups of microorganisms such as bacteria, yeast and fungi are shown at below pH 6 because of the positive charge on the C-2 of the glucosamine monomer.

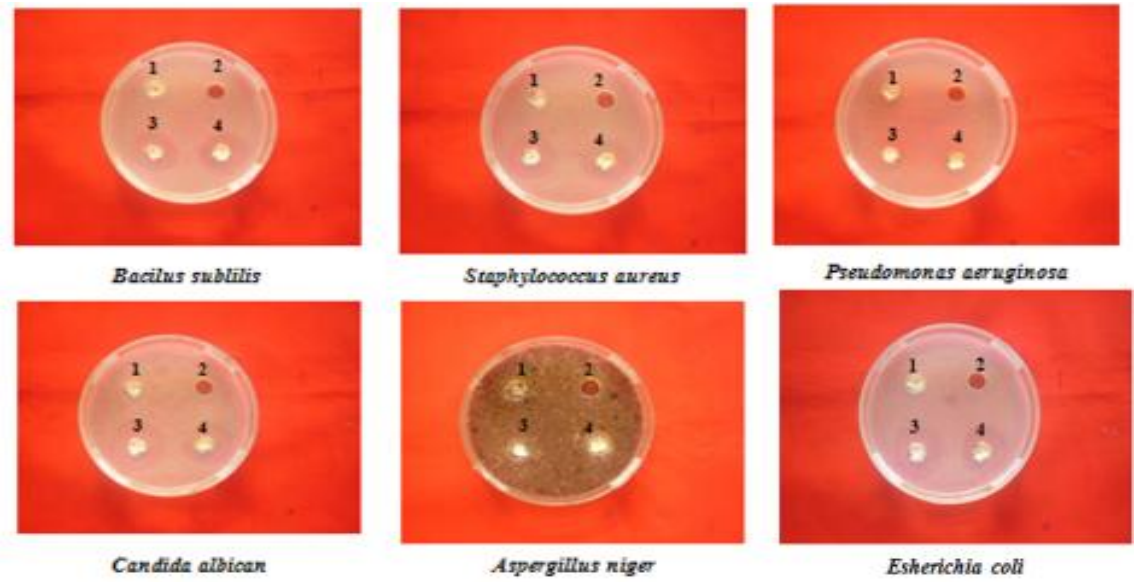

Figure 9 Antimicrobial activities of chitosan, ZnO nanoparticle and the prepared chitosan-ZnO nanocomposite

Table 4 Antimicrobial Activities of CS, ZnO NP's and Obtained CS-ZnO Nanocomposit against Pathogenic Bacteria and Fungi Strains

No.	Samples	Diameter of Inhibition Zone (nm)					
		Bacterial strains				Fungi strains	
		I	II	III	IV	V	VI
1	CS (pH = 7)	-	-	-	-	-	-
2	CS (pH = 9)	12 mm (+)	12 mm (+)	13 mm (+)	13 mm (+)	12 mm (+)	11 mm (+)
3	ZnO NP's	15 mm (++)	25 mm (+++)	26 mm (+++)	24 mm (+++)	13 mm (+)	28 mm (+++)
4	CS-ZnO nanocomposite	15 mm (++)	25 mm (+++)	25 mm (+++)	22 mm (+++)	12 mm (+)	30 mm (+++)

Organisms

I = *Pseudomonas aeruginos* (N. C. T. C-6749)
II = *Esherichia coli* (N. C. I. B-8134)
III = *Staphylococcus aureus* (N. C. P. C-6371)
IV = *Bacillus subtillis* (N. C. I. B-8982)
V = *Aspergillus niger*
VI = *Candida albicans*

Agar well – 10 mm
10 mm ~ 14 mm (+) - lower activity
15 mm ~ 19 mm (++) - higher activity
20 mm ~ above (++) - higher activity

In this research, the prepared chitosan do not show antimicrobial activities at pH 7. The chitosan was also used in the food industry as a food quality enhancer in certain countries. Dietary cookies, potato chip and noodles were produced with chitosan because of its hypocholesterolemic effect. Furthermore, vinegar products containing chitosan are manufactured and sold in Japan again because of their cholesterol lowing ability (Hirano, 1989). The prepared chitosan at pH 9 shows lowest antimicrobial activities were observed against pathogenic bacterial and pathogenic yeast and fungi.

The ZnO nanoparticle showed at highest antimicrobial activity is observed against *Esherichia coli, Staphylococcus aureus, Bacillus subtilis* and *Candida albicans.* The ZnO nanoparticle has moderated effect on *Pseudomonas aeruginosa* and lowest activity on *Aspergillus niger.*

In this research, the prepared CS-ZnO nanocomposite showed highest antimicrobial activity was observed against *Candida albicans.*

Conclusion

In this research, the chitosan was prepared from *Metapenaeus dobosoni* species shrimp shell wastes by using chemical method. The degree of acetylation and the average crystallite size of chitosan are 72% and 12.20 nm, respectively. The yield present of chitosan was 27.82 %. It was completely dissolved in 2% acetic acid. By using AOAC method, the investigation of moisture and ash presents of chitosan were observed 8.6 % and 0.2 %, respectively. The SEM micrograph of chitosan showed the layers of flakes, porous and cage like morphology. Then, the ZnO nanoparticle was prepared by co-precipitation method. In XRD data, Miller indices of the prepared ZnO nanoparticle was matched with ZnO from JCPDF standard library data 80-0075. The average crystallite size of prepared ZnO nanoparticle was 20.99 nm. And then, chitosan-ZnO nanocomposite was prepared by co-precipitation method. The prepared chitosan-ZnO nanocomposite was characterized by FT IR, XRD and SEM measurements. The average crystallite size of prepared chitosan-ZnO nanocomposite was 13.78 nm. The SEM micrograph of prepared chitosan--ZnO nanocomposite showed cage like morphology and uniforming dispersion of ZnO into chitosan. In this research, the antimicrobial activities of the prepared chitosan, prepared ZnO nanoparticle and the prepared chitosan-ZnO nanocomposite were compared. As a results, the prepared ZnO nanoparticle and the prepared chitosan-ZnO nanocomposite showed the highest antimicrobial activities were observed. But the prepared chitosan-ZnO nanocomposite was more effective than ZnO nanoparticle on yeast. Therefore, the prepared chitosan-ZnO nanocomposite can be used in sunscreens, plastic and rubber manufacturing, food, packaging, medical care as well as healthcare, etc. The progress in synthesis of nanoparticles and nanocomposites can be paved the way on the innovative approaches for development of novel antimicrobial agents.

Acknowledgements

The authors would like to express our sincere gratitude to headmaster Dr Kyaw Thu Ya (Technological University, Pathein) for his kind provision of our research Facilities. This work was financially supported by Dr Ye Myint Aung, Professors, Department of Chemistry, Pathein University. Special thanks are due to the Department of Higher Education (Yangon Office), Ministry Education, Yangon, Myanmar. Thanks are also extended to the Myanmar Academy of Arts and Science, Yangon, Myanmar, for allowing submitting this research paper.

References

Arafat, A., S. A. Samad, S. M. Masum and M. Moniruzzaman. (2015). "Preparation and Characterization of Chitosan from Shrimp Shell Waste". *Int. J. Sci & Engi. Res.*,vol. 6, pp.538

Bui, V. K. H., D. Park and Y. C. Lee. (2017). "Chitosan Combined with ZnO, TiO_2 and Ag Nanoparticles for Antimicrobial Wound Healing Applications : A Mini Review of the Research Trends". *Journal Polymer*, vol. 9 (21), pp.1-24

Chung, Y. C., C. L. KuO and C. C. Chen. (2005). "Preparation and Important Functional Properties of Water-Soluble Chitosan Produced Through Millard Reaction". *Bioresource Technology*, vol. 96, pp. 1473-1482

Demir, D., F. Ofkeli, S. Ceylan and N. B. Karagulle. (2016). "Extraction and Characterization of Chitin and Chitosan from Blue Crab and Synthesis of Chitosan Cryogel Scaffolds". *JOTCSA.*, vol,3 (3), pp. 131-144

Dhanavel, S., E.A.K. Nivethaa, V. Narayanan and A. Stephen. (2014). "Photocatalytic activity of Chitosan/ZnO Nanocompositess for Degrading Methylene Blue". *International Journal of Chem Tech Research*., vol. 6 (3), pp.1880-1882

Espitia, P. J. P., N. F. F. Soares, J. S. A. Coimbra, N. J. Andrade, R. S. Cruz and E. A. A. Medreiros. (2012). "Zinc Oxide Nanoparticles : Synthesis, Antimicrobial Activity and Food Packaging Applications". *Food Bioprocess Technol.,* vol. 5, pp.1447-1464

Hirano, S. (1989). *Production and Application of Chitin and Chitosan in Japan in Chitin and Chitosan*. London: *Elsevier Applied Science,* UK, pp. 51-69

Kavitha, A. L. and A. Subashini. (2015)."Synthesis and Characterization of Iron oxide- Chitosan for Dye Decolourization" *Int.J. Adv. Chem.Sci.Appl.,* vol. 3(1), pp. 20-23

Knidri, H. E., R. Belaabed, R. E. Khalfaouy, A. Laajeb, A. Addaou and A. Lahsini. (2017). "Physicochemical Characterization of Chitin and Chitosan Produced from *Parapenacus longirostris* Shrimp Shell Wastes". *Journal of Materials and Environmental Sciences*, vol. 8 (10), pp. 3648 – 3653

Kumar, H. and R. Rani. (2013). "Structural and Optical Characterization of ZnO Nanoparticles Synthesized by Microemulsion Route". *Int. Lett.Chem. Phys. Astronomy.*, vol. 14, pp. 26-36

Kumari, S., P. Rath and S. H. Kumar. (2016). "Chitosan from Shrimp Shell (*Crangon crangon*) and Fish Scales (*Labeorohita*) : Extraction and Characterization". *African Journal of Biotechnology*, vol. 15 (24), pp. 1258-1268

Pokhrel, S., P. N. Yadav and R. Adhikaril. (2015). "Application of Chitin and Chitosan in Industry and Medical Science : A Review". *Nepal Journal of Science and Technology*, vol. 16 (1), pp. 99-104

Salahudin, N. A., M. E. Kemary and E. M. Ibrahim, (2015). "Synthesis and Characterization of ZnO Nanoparticles via Precipitation Method: Effect of Annealing Temperature on Particle Size". *Nanoscience and Nanotechnology*, vol. **5** (4), pp. 82-88

Younes, I. and M. Rinaudo. (2015). "Chitin and Chitosan Preparation from Marine Sources Structures, Properties and Applications". *Mar. Drugs.*,vol. 13, pp.1133-1174